Myoglobin Mutants Giving the Largest Geminate Yield in CO Rebinding in the Nanosecond Time Domain

Takaki Sugimoto,* Masashi Unno,# Yoshitsugu Shiro,§ Yi Dou,¶ and Masao Ikeda-Saito¶

*Faculty of Science, Gakushuin University, Mejiro, Toshima-ku, Tokyo 170, Japan; #Institute for Chemical Reaction Science, Tohoku University, Sendai 980-8577, Japan; §Institute of Physical and Chemical Research (RIKEN), Wako, Saitama 351-01, Japan; and ¶Department of Physiology and Biophysics, Case Western Reserve University School of Medicine, Cleveland, Ohio 44106-4970 USA

ABSTRACT We have measured the rebinding of carbon monoxide (CO) to some distal mutants of myoglobin (Mb) in the time range from 10^{-8} to 10^{-1} s by flash photolysis, in which the photodissociated CO rebinds to the heme iron without escaping to the solvent water from the protein matrix. We have found that the double mutants [$His^{64}\rightarrow Val/Val^{68}\rightarrow Thr$ (H64V/V68T) and $His^{64}\rightarrow Val/Val^{68}\rightarrow Ser$ (H64V/V68S)] have an extremely large geminate yield (70–80%) in water at 5°C, in contrast to the 7% of the geminate yield of wild-type Mb. The CO geminate yields for these two mutants are the largest in those of Mb mutants reported so far, showing that the two mutants have a unique heme environment that favors CO geminate rebinding. Comparing the crystal structures and ^{1}H-NMR and vibrational spectral data of H64V/V68T and H64V/V68S with those of other mutants, we discuss factors that may control the nanosecond geminate CO rebinding and CO migration in the protein matrix.

INTRODUCTION

The geminate ligand rebinding processes are observed in flash photolysis experiments of many hemoproteins, including myoglobin (Mb) and hemoglobin (Hb). In the geminate process, the photodissociated ligand, such as CO, NO, and O_2, remaining in either the heme pocket or the protein matrix rebinds to the heme iron without escaping to the solvent region. The geminate process is directly relevant to the protein dynamic process in the ligand binding reaction, because the structures of Mb and Hb are packed, and dynamic conformational fluctuations must take place for the ligand to migrate between the heme pocket and the solvent water. Therefore, studies on the geminate reaction process provide useful information on the relationship of the protein dynamic fluctuation with ligand diffusion, migration, and rebinding. Many workers have studied the CO geminate process and found that several physical conditions such as temperature and solvent composition alter the kinetic parameters of this process significantly (Lambright et al., 1994; Balasubramanian et al., 1993; Huang and Boxer, 1994; Tian et al., 1993, 1996; Henry et al., 1983; Ansari et al., 1994; Jongeward et al., 1988; Chatfield et al., 1990; Gibson et al., 1986; Carver et al., 1990; Austin et al., 1975; Steinbach et al., 1991). It has been known that heme pocket amino acid replacement also affects the CO geminate process. For example, Carver et al. and later Lambright et al. reported that the Mb single mutants, e.g., $His^{64}\rightarrow Leu$ (H64L) and $Leu^{29}\rightarrow Phe$ (V68F), have relatively large amplitude of the CO geminate rebinding (geminate yield). In addition, Huang and Boxer reported on the basis of the results of the random mutation of Mb that the CO geminate yield is largely affected by the mutation. However, structural factors responsible for the geminate yield, in particular in the nanosecond time range, have yet to be determined. In the present study we have successfully prepared mutant Mbs that exhibit as much as 70% geminate yield in the nanosecond domain and evaluated structural characteristics of the mutants with spectroscopic techniques. From these findings we can gain new insights into the relationships between the protein dynamics and ligand migration in proteins.

Received for publication 11 March 1998 and in final form 27 July 1998.

Address reprint requests to Dr. Yoshitsugu Shiro, Biophysical Chemistry Laboratory, RIKEN Harima Institute, 323-3 Mikazuki-cho, Mihara, Sayo, Hyogo 679-5143, Japan. Tel.: 81-07915-8-2817; Fax: 81-07915-8-2818; E-mail: yshiro@postman.riken.go.jp.

Dr. Dou's present address is Department of Biochemistry and Cell Biology, Rice University, Houston, TX 77005-1892.

0006-3495/98/11/2188/07 $2.00

EXPERIMENTAL PROCEDURES

Mutants of myoglobin

The recombinant sperm whale Mb was expressed in *E. coli* (AR68) with a newly constructed expression system (Dou, 1997), which was based on a modified synthetic gene of Springer and Sligar (1987) and an expression vector, pLcIICFX (Nagai and Thogersen, 1984; Varadarajan et al., 1985). Mb proteins, which have a proper amino acid at position 122 (Asp) without the initiator Met, were isolated and purified as described previously (Ikeda-Saito et al., 1991). Samples for the flash photolysis experiments were 10 μM protein in 0.1 M potassium phosphate buffer in H_2O at pH 7. We did not use a water/glycerol mixture as the solvent.

Flash photolysis measurements

The flash photolysis experiments were carried out using an instrument constructed by UNISOKU (Osaka, Japan) at 5°C. CO adducts of ferrous Mbs were excited with 6-ns (FWHM) pulses from a Q-switched Nd:YAG laser (Surelite I, Continnum). The beam spot was transformed into an ellipsoid by using a cylindrical lens and allowed to fall onto the quartz window of the sample cell (1 cm). The incident energy was ~10 mJ. The absorption changes were monitored by a CW weak probe light from a 150-W xenon arc lamp passed through a monochromator. The probe wavelength at 440 nm was used for the detection of the absorption change after CO photolysis. The detector was protected from scattered excitation laser light by two blue filters with maximum throughout at 400 nm (Surugaseiki). A photomultiplier (R2949; Hamamatsu Photonics) detected

the transmission, and a Iwatsu DS-8631 oscilloscope digitized the transient signal, which was averaged 256 times. The data were collected with a personal computer (PC9801BX/M2; NEC) that set the time domain for the oscilloscope and accumulated the signals. The transmitted intensities I_t at time t were converted to absorbance change ΔA_t with the equation $\Delta A_t = -\log_{10}(I_t/I_0)$, where I_0 is the transmitted intensity before the excitation pulse. Zero time was taken to correspond to the maximum of the absorbance difference. The data were then averaged on a log scale from 5120 to 7680 points.

Resonance Raman and ^{1}H-NMR spectral measurements

The resonance Raman spectra of the Mbs in the deoxy and the CO bound states were measured with a JASCO NR-18000 spectrometer equipped with a liquid nitrogen cooled CCD detector, excited at 441 nm from a He-Cd vapor laser (Kimmon Elect. Co., Saitama, Japan) and at 407 nm from a krypton ion laser (Innova90; Coherent). ^{1}H-NMR spectra of deoxy Mbs were measured at 270 MHz on a Bruker spectrometer at 20°C.

RESULTS AND DISCUSSION

CO rebinding kinetics of H64V, V68T, and H64V/V68T mutants of myoglobin

Fig. 1 illustrates the heme environment of the Mbs employed in this study: wild-type (WT), His^{64}→Val (H64V) (Quillin et al., 1993), Val^{68}→Thr (V68T) (Smerdon et al., 1991; Cameron et al., 1993), and His^{64}→Val/Val^{68}→Thr (H64V/V68T) (Smerdon et al., 1995). We have measured the CO rebinding reaction for these Mbs at 5°C by flash photolysis in a time range of 10^{-8} to 10^{-1} s. Their kinetic traces are shown in Fig. 2 *A*, and the results of the quantitative analysis of the traces are compiled in Table 1. The kinetic features for WT and H64V are essentially the same as those reported previously (Lambright et al., 1994; Tian et al., 1993; Henry et al., 1983; Jongeward et al., 1988), where the CO geminate yields were 7% and 0%, respectively. The substitution of threonine for Val^{68} in WT Mb, i.e., V68T, hardly changed the CO geminate yield (Smerdon et al., 1991). An extremely large CO geminate yield ($I_1 + I_2$; 72%) is observed in H64V/V68T. These results show that the effect of mutation on the CO geminate yield is not additive but is significantly increased upon the substitution of the polar group (-CH(OH)CH$_3$) for the nonpolar isopropyl group (-CH(CH$_3$)$_2$) of Val^{68} in H64V.

To test the effect of introducing a polar group at position 68 in H64V on the CO geminate yield, we have also examined CO rebinding to H64V/V68S and H64V/V68N (Fig. 2 *B*). Ser^{68} has a hydroxyl group as Thr^{68}, and Asn^{68} has a polar amide group. The serine substitution effect on the CO geminate yield is the same as the threonine substitution, as shown in Table 1: 15% for V68S and 71% for H64V/V68S. In contrast, H64V/V68N shows a CO geminate yield of only 14% (Fig. 2 *B*). These results show that the specificity of the OH group at position 68 in H64V is one of the major factors responsible for the large CO geminate yield.

For comparison, the CO rebinding kinetic trace of H64L, which we have measured under the same conditions, is also presented in Fig. 2 *B*. Olson, Boxer and their co-workers have reported an enhanced geminate yield for this mutant (Carver et al., 1990; Lambright et al., 1994; Tian et al.,

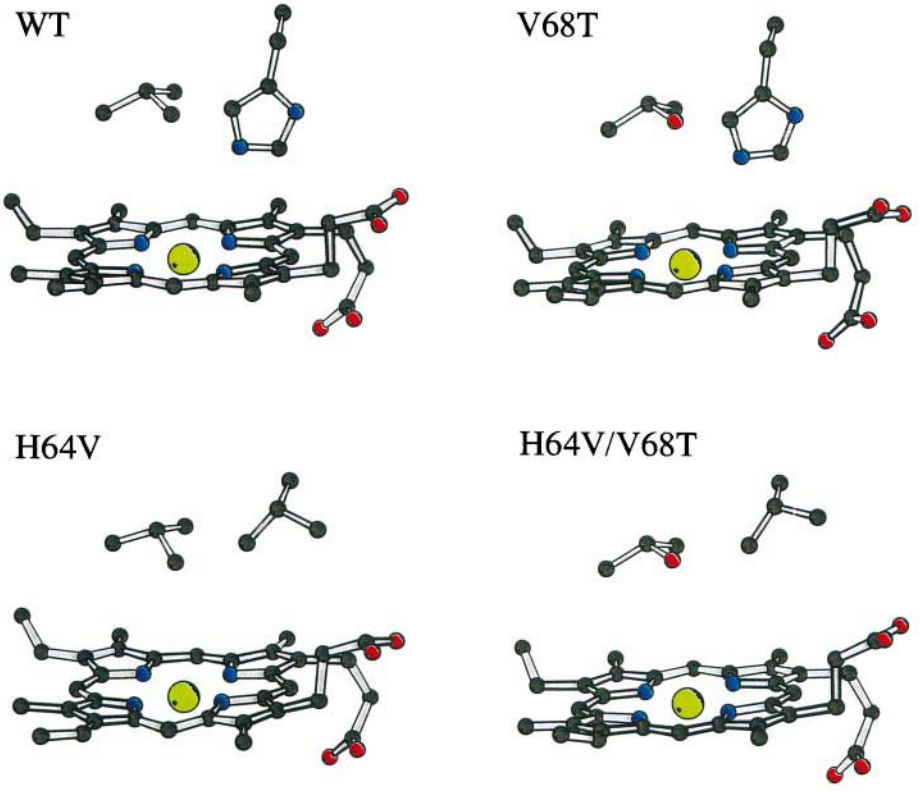

FIGURE 1 Heme environment of WT, H64V, V68T, and H64V/V68T of Mbs in the Met form, determined by x-ray crystallography. The residues at positions 64 and 68 of heme are illustrated. Coordinates of WT, H64V, V68T, and H64V/V68T of Mbs were taken from PDB, whose code numbers are 1vxf, 2 mgj, 1myj, and 1mnk, respectively.

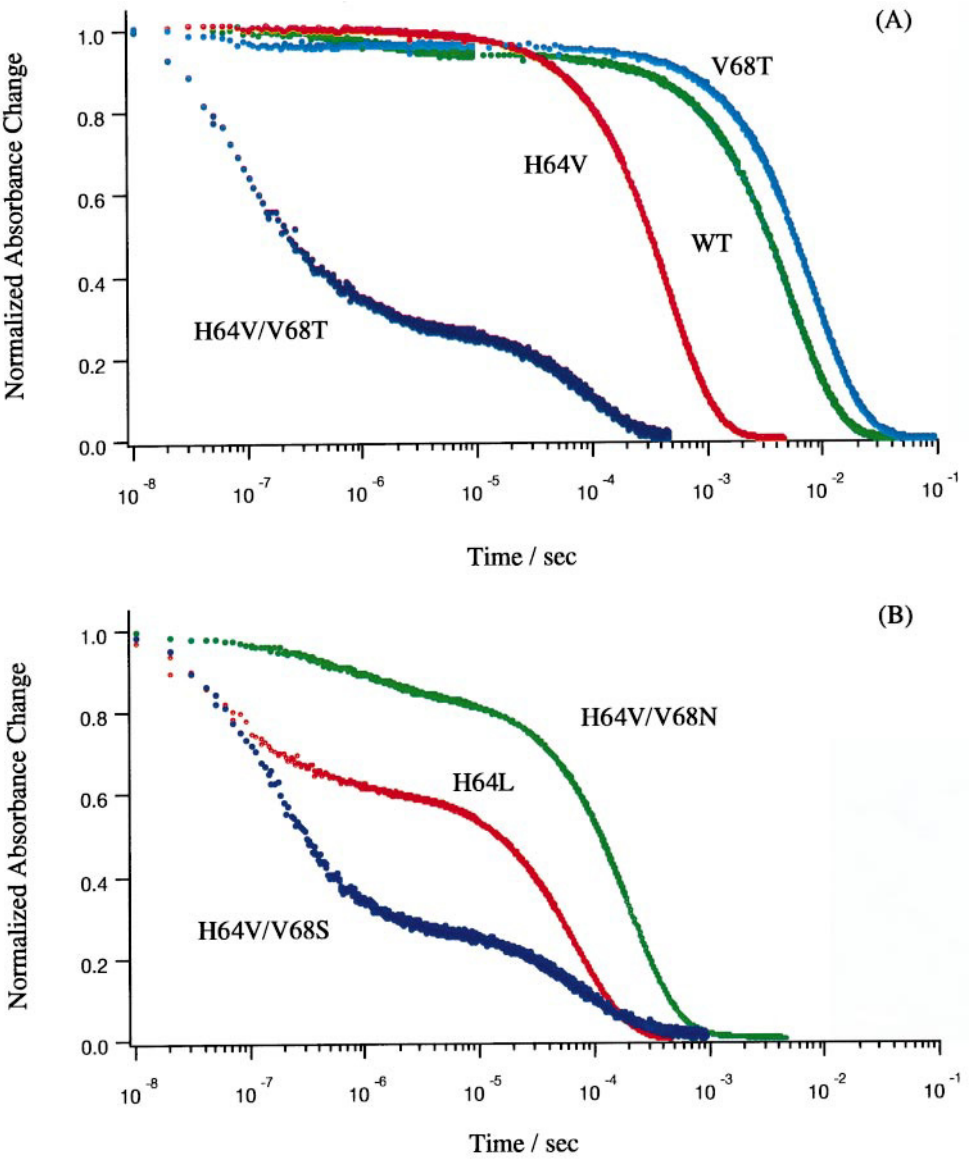

FIGURE 2 (*A*) Kinetic traces of the CO rebinding for WT, H64V, V68T, and H64V/V68T measured in aqueous solution at pH 7 and 5°C. (*B*) Kinetic traces of the CO rebinding for H64V/V68S, H64V/V68N, and H64L measured in aqueous solution at pH 7 and 5°C .

1996). Inspection of Fig. 2 shows how large the CO geminate yields are in H64V/V68T and H64V/V68S, compared with those of other mutants. Many workers have measured the CO flash photolysis of a large number of distal mutants of Mb (Lambright et al., 1994; Huang and Boxer, 1994; Carver et al., 1990; Smerdon et al., 1991, 1995; Cameron et al., 1993). We, too, have measured those for H64F, V68N, H64V/V68I, and H64V/T67R/V68I, where the residues responsible for the bimolecular CO binding reaction have been modified. From this study, we conclude that Val^{64} and Thr/Ser^{68} are the best couple rendering the largest CO geminate yield at present.

To simply represent the effect of the Val^{68} mutation of H64V, we compare the energy diagrams of CO binding for H64V/V68T (large geminate mutant) and H64V/V68N (small geminate mutant) in Fig. 3, which are drawn based on kinetic parameters calculated using the simple sequential model (Carver et al., 1990; Smerdon et al., 1991). The most noticeable difference is that the Mb:CO state, i.e., the first geminate state, relative to the MbCO state is energetically more unstable in H64V/V68T than in H64V/V68N, and that the most inner energy barrier from Mb:CO to MbCO states is significantly lower in H64V/V68T than in H64V/V68N. Because of the relatively unstable Mb:CO state and the lower inner energy barrier, CO rebinding from the protein inside (the Mb:CO state) should be facilitated, causing a larger CO geminate yield for H64V/V68T than for H64V/V68N.

Structural information on the mutants

To examine the large CO geminate yield of H64V/V68T and H64V/V68S in structural terms, we have measured their ^{1}H-NMR and resonance Raman spectra in the deoxy state and compared them with those of other mutants (Table 1).

TABLE 1 Kinetic parameters of the CO rebinding reaction for Mb mutants, the ν(CO) in their ferrous CO forms, and the ^{1}H-NMR chemical shift of His^{93} NH in their deoxy forms

	Geminate 1 $k_{g1} \times 10^{-7}$ (s^{-1}) [I_1 (%)]	Geminate 2 $k_{g2} \times 10^{-6}$ (s^{-1}) [I_2 (%)]	Bimolecular $k_{on} \times 10^{-5}$ (M^{-1} s^{-1}) [I_b (%)]	Main ν(CO) (cm^{-1})	Proximal His NH for deoxy form (ppm)
WT	—	1.1 [7%]	1.14 [93%]	1944*	77.8§
H64V	—	—	16 [100%]	1966*	86.8§
V68T	1.6 [5%]	—	0.90 [95%]	1961*	78.3#
H64V/V68T	0.91 [55%]	0.87 [17%]	71 [28%]	1984*	81.8#
V68S	0.43 [8%]	0.20 [7%]	1.6 [85%]	1945*	77.5#
H64V/V68S	0.57 [57%]	0.79 [14%]	52 [29%]	1976#	80.0#
H64V/V68N	0.74 [3%]	0.98 [11%]	36 [86%]	1933#	79.5#
H64L	1.5 [30%]	2.2 [9%]	110 [61%]	1965*	88.5§

$N(t) = I_1\exp[-k_{g1}t] + I_2\exp[-k_{g2}t] + I_b\exp[-k_bt]$, where k_{g1} and k_{g2} are the rate constants for the fast and slow geminate processes, k_b is the observed first-order rate constant for the bimolecular association process, and I_{g1}, I_{g2}, and I_b are the fractions of the fast geminate, slow geminate, and bimolecular processes, respectively. Kinetic data were obtained at 5°C, and resonance Raman and ^{1}H-NMR spectra were measured at 20°C.

*Smerdon et al. (1991).

#This work.

§La Mar et al. (1994).

The stretching band of the Fe-N_{His93} bond is located at 220 ± 1 cm^{-1} for all of the mutants studied here, indicating that the proximal structure is the same among the Mb mutants, and that the difference in the CO geminate yield comes from structural differences in the distal pocket. The proximal His^{93} NH signals in the ^{1}H-NMR spectra of our mutants, except for H64V, are located relatively in the high-field region. La Mar et al. (1994) showed that the

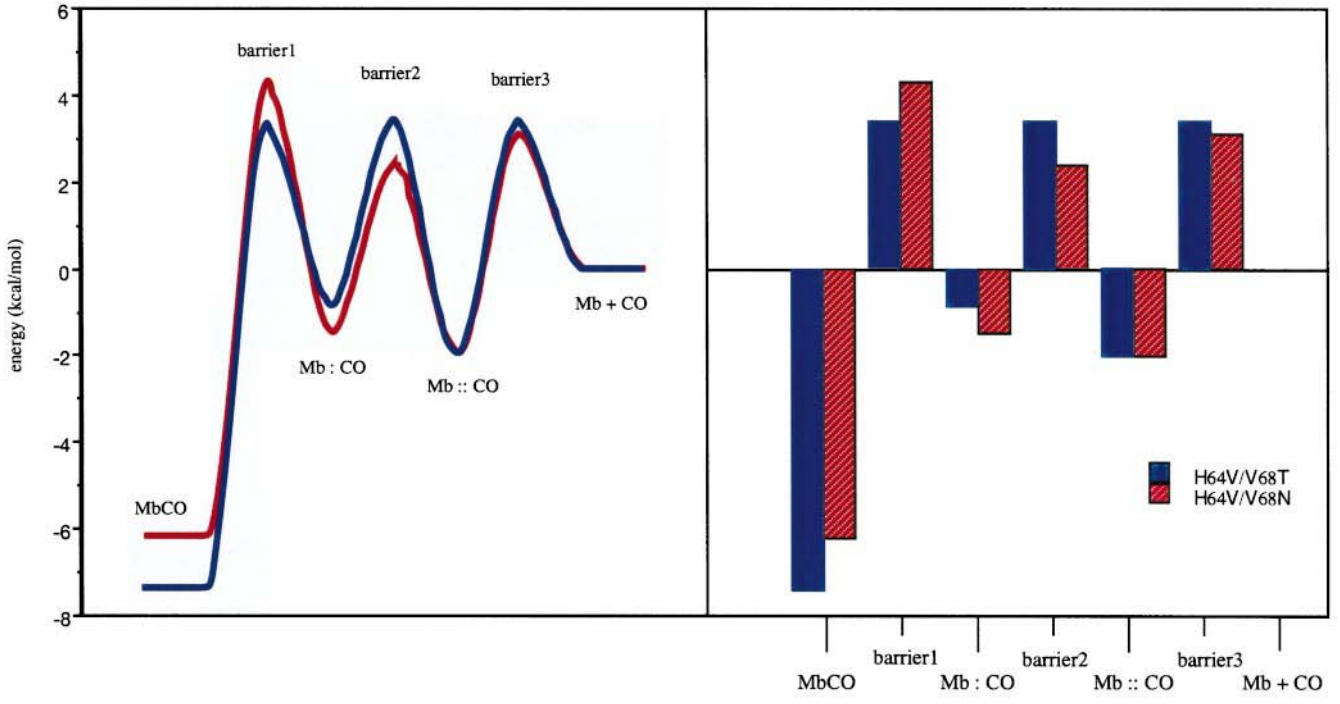

FIGURE 3 Energy diagrams for CO binding to H64V/V68T and H64V/V68N. Free energies were calculated according to the method of Carver et al. (1990). To compare the effect of the amino acid substitution, we used a simple four-state model as the sequential model: MbCO ↔ Mb:CO ↔ Mb::CO ↔ Mb + CO

proximal His^{93} NH signal position in deoxy (ferrous) hemoproteins is sensitive to the presence or absence of the noncoordinated water molecule in the distal heme pocket. According to their suggestion, the present NMR result shows a hydrophilic environment in the distal heme pocket of H64V/V68T and H64V/V68S. As evaluated by x-ray crystallography (see Fig. 1), a comparison of the distal heme pocket structure, especially between H64V and H64V/V68T, clearly shows that the side-chain volume of the residue at position 68 is not the major factor in controlling the CO geminate yield, but that the presence of the nonbonding paired electrons from the O atom of the polar -OH group at position 68 adjacent to the iron-bound CO is responsible for the large CO geminate yield.

We especially consider the stretching frequency of the iron-bound CO, ν(CO), which is now recognized as the index for an environment of the bound-CO in the heme pocket. The ν(CO) of V68T is located at a position (1965 cm^{-1}) (Cameron et al., 1993) different from that of H64V/V68T (1984 cm^{-1}), despite the similarity of the static structure in the immediate vicinity of the iron-bound CO. This is also true for V68S (1947 cm^{-1}) and H64V/V68S (1976 cm^{-1}) (Li et al., 1994) (Table 1). Furthermore, a comparison of H64V/V68T and H64V/V68S to H64V/V68N shows that the former two mutants give a large CO geminate yield, whereas the latter does not, although they all have a polar residue at position 68 and Val at position 64. We observe the ν(CO) of H64V/V68N at 1933 cm^{-1} (Table 1). Therefore, the nonbonding paired electron of the O atom at position 68 and the nonpolar small (Val) residue at position 64 are the best combination, generating a special environment in the distal heme pocket that eventually influences the energetic state of the CO molecule for the rebinding reaction and reduces the inner kinetic energy barrier.

Ligand rebinding in the nanosecond phase

The ligand rebinding in Mb has been examined with many experimental and theoretical techniques. Recent cryocrystallographic studies of MbCO under light illumination (Teng et al., 1994; Schlichting et al., 1994; Hartmann et al., 1996) and molecular dynamic calculations (Vitkup et al., 1997) have shown that the photodissociated CO is located in the heme pocket. Time-resolved IR studies (Lim et al., 1995, 1997) have suggested the presence of a special site, the so-called docking site, in the distal heme pocket for trapping the photodissociated CO. The docking site is above the pyrrole ring C of the heme and is surrounded by some side chains, including His^{64} imidazole and Val^{68} isopropyl groups. The dissociated CO is initially trapped in this site. Some of the CO molecules immediately rebind to the heme iron, yielding the picosecond geminate phase. Some diffuse from the heme pocket and protein matrix and escape to the solvent water for subsequent bimolecular rebinding, or rebind to the heme iron from the protein matrix in the nanosecond geminate phase. In contrast to the picosecond phase, in which ligands rebind from the immediate vicinity of the iron, the nanosecond phases at room temperature represent the rebinding of ligands from positions located in the protein matrix, but quite far from the iron (Ansari et al., 1994).

Three mechanisms have been reported for enhancement of the ligand (CO, O_2, and NO) geminate recombination (Olson and Phillips, 1996; Gibson et al., 1992): 1) trapping the ligand adjacent to the iron by packing the back of the distal pocket with large residues; 2) eliminating steric hindrance for ligand approach to the iron atom; and 3) enhancing the reactivity of the iron atom by proximal effect. In the case of H64V/V68T and H64V/V68S, mechanism 3 can be clearly ruled out, because their proximal structures are unchanged from the WT protein, as manifested by the Fe-N_{His93} stretching frequency and the proximal His^{93} NH chemical shift.

An example of mechanism 1 is V68F Mb, which shows a relatively large geminate yield for the ligand in the nanosecond time domain (Ikeda-Saito et al., 1993). Because of the large Phe^{68} side chain, the ligand cannot move away from the iron atom. In addition, Peterson et al. (1997) have reported that Hb from the nematode *Ascaris suum* has a moderately large CO geminate yield in the nanosecond time range, but that, upon replacing its B10 Tyr with Phe, the CO geminate yield is dramatically decreased. On the basis of the kinetic observations, B10 Tyr in Hb *Ascaris* was proposed to be involved in making a tight "cage" through a hydrogen bond network, preventing the initial movement of the photodissociated ligand away from the iron atom. This explanation was based on the observation that the $Leu^{29} \rightarrow Phe$ replacement (L29F mutant) increased the geminate yield in the O_2 and NO rebinding in sperm whale Mb (Gibson et al., 1992; Olson and Phillips, 1996). The large Phe^{29} side chain contributes to the "cage." From these results, we could explain the extremely large CO geminate yield in H64V/V68T and H64V/V68S in terms of the tight "cage" in the heme distal pocket. However, in the case of Hb *Ascaris* and L29F, the bimolecular rebinding of CO is relatively slow, because of the energy barrier of the tight "cage." This is in sharp contrast to the observation that the bimolecular CO binding constants, k_{on}, of H64V/V68T and H64V/V68S are larger than those of V68T, V68S, and WT (Table 1). In addition, the ν(CO) of the iron-bound CO of Hb *Ascaris* (1912 cm^{-1}) and L29F (1932 cm^{-1}) are different from those of H64V/V68T and H64V/V68S. Therefore, mechanism 1 seems unlikely for the large CO geminate of H64V/V68T and H64V/V68S.

Carlson et al. (1994) have reported that the CO geminate yield of sperm whale Mb H64G/G68A is as large as those of H64V/V68T and H64V/V68S. The observation for H64G/V68A has been interpreted by mechanism 2 (reduction of the distal pocket steric restraint) on the basis of its crystal structure and molecular dynamics computation. However, mechanism 2 cannot sufficiently explain the large CO geminate yield of H64V/V68T, mainly because the CO geminate yield of H64V is much smaller than that of H64V/

V68T, despite the same size of the heme distal pocket between H64V and H64V/V68T. (This is based on their crystal structures of the Met form, because the crystal structures of H64V/V68T in the deoxy and CO forms are not available.) Another factor controlling the CO geminate yield must be considered.

A noticeable difference in the structure of H64V/V68T from H64V is the hydrogen bond formation between the OH group of Thr^{68} and the main-chain carbonyl of Val^{64} (Smerdon et al., 1995). This hydrogen bond interaction does not change the static structure of the distal heme pocket, but could retard the fluctuation of the side chain of the residue at position 68. The restricted fluctuation of the side chain might effectively inhibit the escape of the photodissociated CO from the distal heme pocket, resulting in an increase in the geminate yield. Alternatively, dynamic interactions between the photodissociated CO and the protein matrix, possibly the side chain of the residue at position 68, are altered in H64V/V68H because of the different dynamics of the side chain. We propose that the double mutation $His^{64} \rightarrow Val$ and $Val^{68} \rightarrow Thr/Ser$ not only reduces the steric constraint in the distal heme pocket, but also alters the dynamic and specific interaction of the photodissociated CO molecule with the protein matrix of the distal heme pocket, thereby affecting the energetic state of the CO ligand and possibly lowering the inner energy barrier (see Fig. 3). In the future it will be necessary to characterize the crystal structures of H64V/V68T in the deoxy and the CO forms and to simulate the fluctuation of the protein matrix of the distal heme pocket upon CO photodissociation by the molecular dynamics calculations.

Here we report an extreme example of the modulation of the geminate yield in the CO rebinding of Mb in the nanosecond time range. Static Mb structure as well as biophysical knowledge accumulated so far cannot completely account for the observed large variations in the CO geminate yield in this time domain. We have found a correlation between the large CO geminate yield and the higher frequency of the iron-bound CO in Mb mutants. These vibrational frequency data indicate that an immediate environment of the bound CO molecule is considerably different between V68T and H64V/V68T, and between V68S and H64V/V68S. Such a difference may reflect alterations in the dynamic, steric, and specific interaction of the dissociated CO molecule with the residues in the distal heme pocket or in the protein matrix. However, this finding is insufficient in explaining the nanosecond geminate yield at the molecular and atomic levels. Compared with the picosecond phase, where the movement and location of photodissociated ligands in Mb are well established by experiments and theories, what happens in the nanosecond time frame is not clear. The mutants we have made, H64V/V68T and H64V/V68S, allow us to experimentally evaluate ligand binding of Mb in the nanosecond domain.

We thank Prof. John S. Olson (Rice University) for H64V/T67R/V68I Mb, Ms. Grace C. Chu for her comments, and Prof. Anthony Willkinson (University of York) for pig Mb genes, which were used in the initial phase of the present study. We also thank the reviewers of this manuscript for their informative suggestions.

REFERENCES

Ansari, A., C. M. Jones, E. R. Henry, J. Hofrichter, and W. A. Eaton. 1994. Conformational relaxation and ligand binding in myoglobin. *Biochemistry.* 33:5128–5145.

Austin, R. H., K. W. Beeson, L. Eisenstein, H. Frauenfelder, and I. C. Gunsalus. 1975. Dynamics of ligand binding to myoglobin. *Biochemistry.* 14:5355–5373.

Balasubramanian, S., D. G. Lambright, M. C. Marden, and S. G. Boxer. 1993. CO recombination to human myoglobin mutants in glycerol-water solutions. *Biochemistry.* 32:2202–2212.

Cameron, A. D., S J. Smerdon, A. J. Wilkinson, J. Habash, J. R. Helliwell, T. Li, and J. S. Olson. 1993. Distal pocket polarity in ligand binding to myoglobin: deoxy and carbonmonoxy forms of a threonine 68(E11) mutant investigated by x-ray crystallography and infrared spectroscopy. *Biochemistry.* 32:13061–13070.

Carlson, M. L., R. Regan, R. Elber, H. Li, G. N. Phillips, Jr., J. S. Olson, and Q. H. Gibson. 1994. Nitric oxide recombination to double mutants of myoglobin: role of ligand diffusion in a fluctuating heme pocket. *Biochemistry.* 33:10597–10606.

Carver, T. E., R. J. Rohlfs, J. S. Olson, Q. H. Gibson, R. S. Blackmore, B. A. Springer, and S. G. Sligar. 1990. Analysis of the kinetic barriers for ligand binding to sperm whale myoglobin using site-directed mutagenesis and laser photolysis. *J. Biol. Chem.* 265:20007–20020.

Chatfield, M. D., K. N. Walda, and D. Magde. 1990. Activation parameters for ligand escape from myoglobin proteins at room temperature. *J. Am. Chem. Soc.* 112:4680–4687.

Dou, Y. 1997. Protein engineering reveals specific roles of amino acid residues in function and stability of myoglobin. Ph.D. thesis, Case Western Reserve University.

Gibson, Q. H., J. S. Olson, R. E. McKinnie, and R. J. Rohlfs. 1986. A kinetic description of ligand binding to sperm whale myoglobin. *J. Biol. Chem.* 261:10228–10239.

Gibson, R. H., R. Regan, R. Elber, J. S. Olson, and T. E. Carver. 1992. Distal pocket residues affect picosecond ligand recombination in myoglobin: an experimental and molecular dynamics study of position 29 mutants. *J. Biol. Chem.* 267:22022–22034.

Hartmann, H., S. Zinser, P. Komninos, R. T. Shneider, G. U. Nienhaus, and F. Parak. 1996. X-ray structure determination of a metastable state of carbonmonoxy myoglobin after photodissociation. *Proc. Natl. Acad. Sci. USA.* 93:7013–7016.

Henry, E. R., J. H. Sommer, J. Hofrichter, and W. A. Eaton. 1983. Geminate recombination of carbon monoxide to myoglobin. *J. Mol. Biol.* 166:443–451.

Huang, X., and S. G. Boxer. 1994. Discovery of new ligand binding pathway in myoglobin by random mutagenesis. *Nature Struct. Biol.* 1:226–229.

Ikeda-Saito, M., Y. Dou, T. Yonetani, J. S. Olson, T. Li, R. Regan, and Q. H. Gibson. 1993. Ligand diffusion in the distal pocket of myoglobin: a primary determination of geminate rebinding. *J. Biol. Chem.* 268: 6855–6857.

Ikeda-Saito, M., R. S. Lutz, D. A. Shelly, E. J. MaKelvey, R. Mattera, and H. Hori. 1991. EPR characterization of the stereochemistry of the distal heme pocket of the engineered human myoglobin mutants. *J. Biol. Chem.* 266:23641–23647.

Jongeward, K. A., D. Magde, D. J. Taube, J. C. Marsters, T. G. Traylor, and V. S. Sharma. 1988. Picosecond and nanosecond geminate recombination of myoglobin with CO, O_2, NO. *J. Am. Chem. Soc.* 110: 380–387.

La Mar, G. N., F. Dailichow, X. Zhao, Y. Dou, M. Ikeda-Saito, M. L. Chiu, and S. G. Sligar. 1994. ^1H NMR investigation of distal mutant deoxy myoglobins. Interpretation of proximal His contact shifts in terms of a localized distal water molecule. *J. Biol. Chem.* 269:29629–29635.

Lambright, D. G., S. Balasubramanian, S. M. Decatur, and S. G. Boxer. 1994. Anatomy and dynamics of a ligand-binding pathway in

myoglobin: the roles of residues 45, 60, 64, and 68. *Biochemistry.* 33:5518–5525.

Li, T., M. L. Quillin, G. N. Phillips, Jr., and J. S. Olson. 1994. Structural determinants of the stretching frequency of CO bound to myoglobin. *Biochemistry.* 33:1433–1446.

Lim, M., T. A. Jackson, and P. A. Anfinrud. 1995. Binding of CO to myoglobin from a heme pocket docking site to form nearly linear Fe-C-O. *Science.* 269:962–966.

Lim, M., T. A. Jackson, and P. A. Anfinrud. 1997. Ultrafast rotation and trapping of carbon monoxide dissociated from myoglobin. *Nature Struct. Biol.* 4:209–214.

Nagai, K., and H. C. Thogensen. 1984. Synthesis and sequence-specific proteolysis of hybrid proteins produced in *Escherichia coli. Methods Enzymol.* 153:461–481.

Olson, J. S., and G. N. Phillips, Jr. 1996. Kinetic pathways and barriers for ligand binding to myoglobin. *J. Biol. Chem.* 271:17593–17596.

Peterson, E. S., S. Huang, J. Wang, L. M. Miller, G. Vidugiris, A. P. Kloek, D. E. Goldberg, M. R. Chance, J. B. Wittenberg, and J. M. Friedman. 1997. A comparison of functional and structural consequences of the tyrosine B10 and glutamine E7 motifs in two invertebrate hemoglobins (*Ascaris suum* and *Lucina pectinata*). *Biochemistry.* 36:13110–13121.

Quillin, M. L., R. M. Arduini, J. S. Olson, and G. N. Phillips, Jr. 1993. High-resolution crystal structures of distal histidine mutants of sperm whale myoglobin. *J. Mol. Biol.* 234:140–155.

Schlichting, I., J. Berendzen, G. N. Phillips, Jr., and R. M. Sweet. 1994. Crystal structure of photolysed carbonmonoxy-myoglobin. *Nature.* 317: 808–812.

Smerdon, S. J., A. M. Brzozowski, G. J. Davies, A. J. Wilkinson, A. Brancaccio, F. Cutruzzola, C. Travaglini, M. Brunori, T. Li, R. E. Brantley, Jr., T. E. Craver, R. F. Eich, E. Singleton, and J. S. Olson. 1995. Interactions among residues CD, E7, E10, and E11 in myoglobins: attempts to simulate the ligand-binding properties of *Aplysia* myoglobin. *Biochemistry.* 34:8715–8725.

Smerdon, S. J., G. G. Dodson, A. J. Wilkinson, Q. H. Gibson, R. S. Blackmore, T. E. Carver, and J. S. Olson. 1991. Distal pocket polarity in ligand binding to myoglobin: structural and functional characterization of a threonine 68(E11) mutant. *Biochemistry.* 30:6252–6260.

Springer, B. A., and S. G. Sligar. 1987. High-level expression of sperm whale myoglobin in *Escherichia coli. Proc. Natl. Acad. Sci. USA.* 84:8961–8965.

Steinbach, P. J., A. Ansari, J. Berendzen, D. Braunstein, K. Chu, B. R. Cowen, D. Ehrenstein, H. Frauenfelder, J. B. Johnson, D. C. Lamb, S. Luck, J. R. Mourant, G. U. Nienhaus, P. Ormos, R. Phillipp, A. Xie, and R. D. Young. 1991. Ligand binding to heme proteins: connection between dynamics and function. *Biochemistry.* 30:3988–4001.

Teng, T. Y., V. Srajer, and K. Moffat. 1994. Photolysis-induced structural changes in single crystals of carbonmonoxy myoglobin at 40K. *Nature Struct. Biol.* 1:701–705.

Tian, W. D., J. T. Sage, and P. M. Champion. 1993. Investigations of ligand association and dissociation rates in the "open" and "closed" states of myoglobin. *J. Mol. Biol.* 233:155–166.

Tian, W. D., J. T. Sage, P. M. Champion, E. Chien, and S. G. Sligar. 1996. Probing heme protein conformational equilibration rates with kinetic selection. *Biochemistry.* 35:3487–3501.

Varadarajan, R., A. Szabo, and S. G. Boxer. 1985. Cloning, expression in *Escherichia coli* and reconstitution of human myoglobin. *Proc. Natl. Acad. Sci. USA.* 82:5681–5684.

Vitkup, D., G. A. Petsuko, and M. Karplus. 1997. A comparison between molecular dynamics and x-ray results for dissociated CO in myoglobin. *Nature Struct. Biol.* 4:202–208.